DMD Fast Forward. Published on March 28, 2014 as doi:10.1124/dmd.114.057620

DMD #57620

Identification of bioactivating enzymes involved in the hydrolysis of laninamivir octanoate, a long-acting neuraminidase inhibitor, in human pulmonary tissue

Kumiko Koyama, Yuji Ogura, Daisuke Nakai, Mihoko Watanabe, Toshiko Munemasa, Yuka Oofune, Kazuishi Kubota, Akira Shinagawa, and Takashi Izumi

Drug Metabolism & Pharmacokinetics Research Laboratories (K.Ko., D.N., T.I.), Daiichi Sankyo Co., Ltd., Tokyo, Japan; Discovery Science and Technology Department, Daiichi Sankyo RD Novare Co., Ltd., Tokyo, Japan (Y.Og., M.W., Y.Of., K.Ku., A.S.); and Translational Medicine and Clinical Pharmacology Department (T.M.), Daiichi Sankyo Co., Ltd., Tokyo, Japan

Running title: Identification of laninamivir octanoate hydrolases

To whom all correspondence should be sent:

Kumiko Koyama

Drug Metabolism & Pharmacokinetics Research Laboratories

Daiichi Sankyo Co., Ltd.

1-2-58, Hiromachi, Shinagawa-ku, Tokyo 140-8710, Japan.

Phone: +81-3-3492-3131, Fax: +81-3-5436-8567

E-mail: koyama.kumiko.hv@daiichisankyo.co.jp

Kazuishi Kubota

Discovery Science and Technology Department

Daiichi Sankyo RD Novare Co., Ltd.

1-16-13, Kitakasai, Edogawa-ku, Tokyo 134-8630, Japan.

Phone: +81-3-5696-8301, Fax: +81-3-5696-3548

E-mail: kubota.kazuishi.ci@rdn.daiichisankyo.co.jp

DMD Fast Forward. Published on March 28, 2014 as DOI: 10.1124/dmd.114.057620
This article has not been copyedited and formatted. The final version may differ from this version.

Number of text pages: 36

Number of tables: 3

Number of figures: 6

Number of references: 44

Number of words in abstract: 234 words

Number of words in introduction: 616 words

Number of words in discussion: 1142 words

Abbreviations: APT1, acyl-protein thioesterase 1; BNPP, bis-*p*-nitrophenyl phosphate; BSA, bovine serum albumin; DFP, diisopropyl fluorophosphate; DTNB, 5,5'-dithiobis(2-nitrobenzoic acid); ELF, epithelial lining fluids; ESD, esterase D; IS, internal standard; LO, laninamivir octanoate; NP-40; Nonidet P-40

DMD Fast Forward. Published on March 28, 2014 as DOI: 10.1124/dmd.114.057620
This article has not been copyedited and formatted. The final version may differ from this version.

Abstract

Laninamivir octanoate (LO) is an octanoyl ester prodrug of the neuraminidase inhibitor laninamivir. After inhaled administration, LO exhibits the clinical efficacy for both treatment and prophylaxis of influenza virus infection, resulting from the hydrolytic bioactivation into its pharmacologically active metabolite laninamivir in the pulmonary tissue. In this study, we focused on the identification of LO-hydrolyzing enzymes from human pulmonary tissue extract, using proteomic correlation profiling — a technology integration of traditional biochemistry and proteomics. In a single elution step by gel filtration chromatography, LO-hydrolyzing activity was separated into two distinct peaks, designated as peak I and peak II. By mass spectrometry, 1160 and 1003 proteins were identified and quantitated for peak I and peak II, respectively, and enzyme candidates were ranked based on the correlation coefficient between the enzyme activity and the proteomic profiles. Among proteins with a high correlation value, S-formylglutathione hydrolase (esterase D; ESD) and acyl-protein thioesterase 1 (APT1) were selected as the most likely candidates for peak I and peak II, respectively, which was confirmed by LO-hydrolyzing activity of recombinant proteins. In the case of peak II, LO-hydrolyzing activity was completely inhibited by treatment with a specific APT1 inhibitor, palmostatin B. Moreover, immunohistochemical analysis revealed that both enzymes were mainly localized in the pulmonary epithelia, a primary site of influenza virus infection. These findings demonstrate that ESD and APT1 are key enzymes responsible for the bioactivation of LO in human pulmonary tissue.

Introduction

Laninamivir octanoate (LO), an octanoyl ester prodrug of the neuraminidase inhibitor laninamivir, demonstrates a long-lasting antiviral effect in contrast to oseltamivir and zanamivir, and is currently used in clinical practice in Japan for treatment and prophylaxis of influenza virus infection. In confirmatory clinical trials, a single inhalation of LO demonstrated a therapeutic efficacy in both adult and pediatric patients (Sugaya et al. 2010, Watanabe et al. 2010, Watanabe et al. 2013). In addition, LO was recently reported to be efficacious in the post-exposure prophylaxis of influenza in household contacts (Kashiwagi et al. 2013).

Hydrolytic activation of LO into the active form laninamivir in the pulmonary tissue is a critical factor for exerting its *in vivo* pharmacological effect. After a single intranasal/intratracheal administration in mice and rats, LO was efficiently hydrolyzed to laninamivir, and then it was highly retained in the pulmonary tissue (Koyama et al. 2009, Koyama et al. 2010); with a sufficient concentration in the epithelial lining fluids (ELF), a possible site of action of neuraminidase inhibitors (Koyama et al. 2013). In humans as well, after a single inhalation of LO (40 mg), laninamivir was generated and highly maintained in the ELF (Ishizuka et al. 2012), exceeding the *in vitro* 50% inhibitory concentrations for influenza viral neuraminidases over 10 days (Yamashita et al. 2009). A slow elimination of laninamivir was also observed in the systemic circulation, with an elimination half-life ($t_{1/2}$) of approximately 3 days (Ishizuka et al. 2009, Yoshiba et al. 2011). These favorable pharmacokinetic characteristics are considered to result in the long-lasting effect.

In drug development, the prodrug approach has been widely used as a strategy for improving the physicochemical, biopharmaceutical or pharmacokinetic properties of pharmacologically active agents, and approximately 10% of the drugs approved worldwide are reported to be classified as prodrugs (Rautio et al. 2008, Zawilska et al. 2013). Prodrugs require the bioactivation into their active forms by metabolizing enzymes in order to be therapeutically effective. On the other hand, the prodrug-activating enzymes may have a potential risk to influence interindividual variability in drug exposure and response, and possibly to induce drug-drug interactions. Therefore, it is very important to identify the prodrug-activating enzymes.

For the molecular identification of endogenous enzymes from biological samples, biochemical purification has been used for decades as a general methodology, and a series of sequential separation by different chromatographic methods (ion-exchange, affinity, gel filtration, etc.) is usually required to achieve the purification. On the other hand, we have recently extended an advanced methodology named proteomic correlation profiling to identify drug metabolizing enzymes (Sakurai et al. 2013), whose basic concept was previously reported by Kubota et al (2009). In this methodology, the biological material is fractionated by column chromatography, followed by the calculation of each protein's correlation coefficient between the enzyme activity and proteomic profile of the fractions. Subsequently, possible enzyme candidates are chosen among proteins with a high correlation value, based on the fundamental assumption that protein quantity correlates with protein activity. This streamlined method enables us to require fewer purification steps with minimal starting material, and also to resolve the challenges associated with physicochemical stability and solubilization, as compared to the conventional biochemical

purification. Therefore, the proteomic correlation profiling is considered to be a powerful and efficient tool for enzyme identification.

In the present study, from the human pulmonary tissue extract, we identified S-formylglutathione hydrolase (also known as esterase D; ESD) and acyl-protein thioesterase 1 (APT1) as most likely candidates for LO-hydrolyzing enzymes, using the proteomic correlation profiling. We also performed further analysis to confirm the enzyme identification and to investigate the enzyme localization in the pulmonary tissue. We believe that this study can provide fundamental information on the LO bioactivation process in the target site.

Materials and methods

Materials. Both LO and laninamivir were synthesized at Daiichi Sankyo Chemical Pharma Co., Ltd. (Tokyo, Japan) and their chemical structures are illustrated in Fig. 1. The internal standard (IS) of laninamivir ([$^2H_3$]laninamivir) was synthesized at Daiichi Sankyo Co., Ltd. (Tokyo, Japan). Palmostatin B was synthesized at Daiichi Sankyo RD Novare Co., Ltd. (Tokyo, Japan). Pooled human pulmonary subcellular fractions (S9, microsomes, and cytosol), used for LO-hydrolysis characteristics, were obtained from XenoTech, LLC (Lenexa, KS), whereas individual human pulmonary S9 (79-year-old, male), used for gel filtration chromatography, was obtained from Human and Animal Bridging Research Organization (Chiba, Japan). Formalin-fixed and paraffin-embedded human pulmonary tissue sections (62-year-old, male) were obtained from SuperBioChips Laboratories (Seoul, Korea). Ethical approval for these human specimens was obtained from each Research Ethics Committee at Daiichi Sankyo Co., Ltd. and Daiichi Sankyo RD Novare Co., Ltd. Diisopropyl fluorophosphate (DFP) and eserine were purchased from Wako Pure Chemical Industries, Ltd. (Osaka, Japan), whereas bis-*p*-nitrophenyl phosphate (BNPP) and 5,5'-dithiobis(2-nitrobenzoic acid) (DTNB) were purchased from Nacalai Tesque, Inc. (Kyoto, Japan). Recombinant human esterase D (rESD) and acyl-protein thioesterase 1 (rAPT1) were obtained from Novoprotein Scientific Inc. (Shanghai, China). Rabbit anti-ESD and anti-APT1 antibodies were obtained from Sigma-Aldrich Co. (St. Louis, MO) and Proteintech Group, Inc. (Chicago, IL), respectively. All other reagents and solvents used were commercially available and were of extra-pure, guaranteed or LC-MS grade.

DMD Fast Forward. Published on March 28, 2014 as DOI: 10.1124/dmd.114.057620
This article has not been copyedited and formatted. The final version may differ from this version.

LO hydrolysis assay and chemical inhibition properties. For determination of LO-hydrolyzing activity in human pulmonary subcellular fractions (S9, cytosol, and microsomes) and recombinant proteins (rESD and rAPT1), the sample was incubated at 37°C for 15 min with 10 μM LO. The reaction was terminated by mixing with 2-volumes of acetonitrile. The sample was added an aliquot of IS and then filtered. The resulting sample was injected into the liquid chromatography coupled with a tandem mass spectrometry (LC-MS/MS) system consisting of API 4000 (Applied Biosystems, Foster City, CA) coupled to Shimadzu 20A (Shimadzu Corp., Kyoto, Japan). The analyte was separated on an analytical column, a PC HILIC Silica (5 μm, 2.0 × 150 mm; Shiseido Co., Ltd., Tokyo, Japan), with a gradient of 10 mM ammonium acetate and acetonitrile. The flow rate employed was 0.6 ml/min. The analyte was detected with an electrospray ionization (ESI) source operated in the positive-ion mode. MS data were acquired in selected ion multiple reaction monitoring mode using the mass transitions of m/z 347→60 and 350→60 for laninamivir and IS, respectively. The calibration curves were generated using the analyte to IS peak area ratio by weighted (1/x) least-squares linear regression over the concentration ranges of 1–1000 ng/ml (2.89–2890 pmol/ml). The enzymatic activity was expressed as a metabolite formation rate (pmol/min/mg) based on the production of laninamivir. For assay of chemical inhibition properties, each of the esterase inhibitors (DFP, BNPP, eserine, and DTNB) was added to the reaction mixture and further incubated with 10 μM LO. The results were expressed as percentages of the activity in the absence of inhibitors.

DMD Fast Forward. Published on March 28, 2014 as DOI: 10.1124/dmd.114.057620
This article has not been copyedited and formatted. The final version may differ from this version.

Gel filtration chromatography. Human pulmonary S9 fraction (5 mg/ml, 20 mM HEPES; pH 7.0, 250 mM sucrose) was used as a starting material. The S9 fraction (500 μL) was incubated for 10 min, following the addition of 10% Nonidet P-40 (NP-40; 50 μL) and 5 M NaCl (50 μL). After centrifugation at 105,000*g* for 1 h, the supernatant was filtered and loaded onto a gel filtration column Superdex 200 (GE Healthcare UK Ltd.), which was equilibrated with running buffer (20 mM HEPES; pH 7.0, 150 mM NaCl and 0.05% NP-40) at a flow rate of 0.5 ml/min. The protein separation was performed with the same buffer at a flow rate of 0.5 ml/min, and the eluent was collected in a series of fractions at every 1 min. A gel filtration standard (Bio-Rad Laboratories, Inc., Hercules, CA) was used for determination of the molecular weight. All procedures were conducted at 4°C.

LO hydrolysis assay in chromatography fractions. For assay of LO-hydrolyzing activity in the gel filtration chromatographic fractions, an aliquot of sample was incubated at 37°C for 1 h with 420 μM (200 μg/ml) LO. The reaction was terminated by mixing with an equal volume of acetonitrile. The sample was added an aliquot of IS and then filtered. The resulting sample was injected in the liquid chromatography coupled with a mass spectrometry (LC-MS) system consisting of 1200 LC/MSD coupled to 1200SL (Agilent Technologies, Inc., Santa Clara, CA). The analyte was separated on an analytical column, an Asahipak NH2P-50 2D (5 μm, 2.0 × 150 mm; Showa Denko K. K., Tokyo, Japan), with an isocratic mobile phase consisting of 10 mM ammonium acetate/acetonitrile (45:55). The flow rate employed was 0.3 ml/min. The analyte was detected with the ESI source operated in positive-ion mode. MS data were acquired in selected ion monitoring mode at

m/z 347 and m/z 350 for laninamivir and IS, respectively. For APT1 inhibitory assay, the reaction mixture was incubated with 420 μM LO in the presence of 0.1 μM palmostatin B. One unit of LO-hydrolyzing activity was defined as the activity required for 1 nmol/ml production of laninamivir.

Protein identification and quantification in chromatographic fractions. Two hundred fmol of bovine serum albumin (BSA) was added as IS to an aliquot of each fraction from gel filtration chromatography. Then, each fraction was subjected to methanol/chloroform precipitation, in-solution reduction and alkylation, followed by trypsin digestion, in a similar manner with our previous report (Sakurai et al. 2013). In brief, proteins were precipitated with Methanol/Chloroform precipitation (Wessel and Flügge 1984) to remove salts and detergents, then reduced with dithiothreitol followed by alkylation with iodoacetamide, and digested with trypsin. Resulting peptides were desalted with StageTips (Rappsilber et al. 2007) and dissolved with 12 μL of 5% formic acid. An aliquot of the peptide mixtures (4 μL) was injected into the LC-MS/MS system consisting of LTQ-Orbitrap ELITE coupled to Easy-nLC II (Thermo Fisher Scientific Inc., Waltham, MA). The peptides were eluted from the in-house packed tip column (140 mm × 75 μm I.D., 3 μm Inertsil C18, GL Sciences) with a linear gradient of acetonitrile in 0.1% formic acid at a flow rate of 200 nL/min. Protein identification and quantification were performed by the MaxQuant (version 1.2.0.5, Max Planck Institute) (Cox et al. 2009 and 2011). Briefly, MS/MS spectra were searched against UniprotKB/Swiss-Prot human data downloaded on 28 Nov 2012. The identified proteins were quantified in an ion intensity-based label-free algorithm implemented in MaxQuant, which was a relative

quantitation algorithm using the ion intensity of identified peptides in LC-MS without stable isotope labeling technology such as SILAC (Ong et al. 2002), iTRAQ (Ross et al. 2004) or AQUA (Gerber et al. 2003). Two missed cleavages were allowed, along with carbamidomethylation of cysteine as a fixed modification; variable modifications were oxidation of methionine and acetylation of N-term amino acid of the protein. Mass tolerance for precursor ions was 7 ppm, mass tolerance for fragment ions was 0.5 Da, and false discovery rates at peptide and protein levels were less than 0.01. The proteins identified by more than one single peptide were used for further correlation analysis.

Proteomic correlation profiling. Following MaxQuant analysis, all proteins quantified in each fraction were normalized by the amount of BSA to account for any experimental error and to correct any variations in sample complexity. Pearson correlation coefficient was calculated between the normalized abundance profile for each protein and LO-hydrolyzing activity profile.

Protein assay. Total protein concentration was determined by modified Bradford protein assay (Coomassie Plus Protein Assay, Thermo Fisher Scientific, Inc.) using BSA as a standard protein. Chromatographic fractions were assayed before a spike-in of BSA as IS for label-free quantitation.

Immunohistochemistry. Immunohistochemical assay was performed on formalin-fixed, paraffin-embedded human pulmonary tissue sections using Dako Autostainer Link 48 (Dako Denmark A/S, Glostrup, Denmark). Deparaffinization and target retrieval were

processed on the tissue sections in a single step using Dako PT Link (EnVision FLEX TRS Low pH), where the optimal incubation was set at 97°C for 20 min. Endogenous peroxidase activity was quenched with peroxidase-blocking solution (Dako) for 5 min, and nonspecific antibody binding was blocked with protein block, serum-free (Dako) for 30 min. Then, anti-ESD antibody or anti-APT1 antibody (2 μg/ml) was applied as a primary antibody on the sections and incubated for 45 min, and isotype antibody (2 μg/ml) was used as a negative control. EnVision+System-HRP Labelled Polymer Anti-Rabbit was reacted as a secondary antibody for 30 min, and antibody complex was visualized after the addition of 3,3'-diaminobenzidine tetrahydrochloride (DAB)+, liquid (5 min × 2; Dako). The section was counterstained with hematoxylin.

Results

Enzymatic LO hydrolysis in human pulmonary subcellular fractions. LO-hydrolyzing activity in human pulmonary S9, cytosol, and microsomes is shown in Fig. 2A. At 10 μM LO, activity was observed in all of the subcellular fractions tested, with almost the same levels per mg protein basis (1.2-1.9 pmol/min/mg). Furthermore, for the inhibitory effect of typical esterase inhibitors, LO-hydrolyzing activity in pulmonary S9 was strongly inhibited by a potent serine esterase inhibitor DFP at 0.1 mM or more. DTNB, known as an inhibitor of SH-containing esterase, exhibited weaker inhibitory effects than DFP, whereas much weaker inhibition was observed in the treatment with BNPP (carboxylesterase inhibitor). Eserine (cholinesterase inhibitor) showed no enzymatic inhibition (Fig. 2B).

Selection of possible candidate proteins for LO-hydrolyzing enzymes. A schematic diagram for this study is illustrated in Fig. 3. As shown in Fig. 2A, LO-hydrolyzing activity in pulmonary S9 was substantially derived not only from the soluble fraction (cytosol) but also from the insoluble fraction (microsomes). Therefore, non-ionic detergent NP-40 was added to the S9 fraction in order to solubilize membrane proteins without altering biological activity, and the centrifuged soluble fraction (overall recovery: 73.8%) was subjected to a single-step gel filtration chromatography. From enzyme assay for the chromatographic fractions collected, LO-hydrolyzing activity was separated into two distinct peaks (Fig. 4), which were designated as peak I (fraction No. 26-32) and peak II (fraction No. 33-39), respectively. The contribution rate to total activity was estimated to

be approximately 40% and 30% for peak I and peak II, respectively, based on the calculation of each peak area (%) of LO-hydrolyzing activity in the gel filtration fractions. Then, in order to seek proteins that showed a high correlation with LO-hydrolyzing activity, all proteins in the fractions were identified and quantified by LC-MS/MS analysis. Theoretically protein of a higher correlation coefficient has higher probability of a responsible protein to the activity profile and our previous experiences (Kubota et al. 2009, Sakurai et al. 2013, and unpublished results) are in agreement with this concept. In total, 2381 proteins were identified, however there was no single protein that had the bimodal chromatographic peaks highly correlated with the enzyme activity profile (data not shown). Therefore, it was speculated that the active peaks consisted of two individual enzymes, which were independently derived from peak I and peak II. Possible candidate proteins were listed for each peak based on the correlation coefficient with the enzyme activity profile. In respect to peak I, there were 1160 proteins identified, and the top 30 most correlated proteins were listed in Table 1. In a similar manner, with regard to peak II, 1003 proteins were identified and the top 30 proteins were also placed in descending order of correlation coefficient, as shown in Table 2. Among the proteins that were annotated as "hydrolase", ESD (R^2=0.9432) and APT1 (R^2=0.9765) were finally selected as the most possible candidates for the peak I- and peak II-derived proteins, respectively. ESD and APT1 proteins were clearly detected in the peak I and peak II fractions, respectively, by Western blot analysis (data not shown).

Identification of ESD and APT1 as LO-hydrolyzing enzymes. In order to investigate whether both ESD and APT1 are authentic candidates for the LO-hydrolyzing enzymes,

their recombinant proteins (rESD and rAPT1) were subjected to the determination of LO-hydrolyzing activity. As shown in Table 3, the enzyme activities in rESD and rAPT1 were 232±16 and 377±36 pmol/min/mg at 10 μM LO, respectively, both of which were more than 100-fold higher than that in human pulmonary S9 (1.56±0.05 pmol/min/mg). On the other hand, BSA (negative control) had a negligible activity.

Inhibitory effect of palmostatin B on chromatographic LO-hydrolyzing activity. Palmostatin B is known as a specific APT1 inhibitor (Dekker et al. 2010, Rusch et al. 2011), although no specific inhibitor has been reported for ESD. LO-hydrolyzing activity profiles were measured for the fractions separated by gel filtration chromatography, in the absence or presence of a specific APT1 inhibitor, palmostatin B (Fig. 5). In the absence of palmostatin B, there were two active peaks, peak I and peak II, on the chromatogram. On the other hand, in the presence of palmostatin B, peak II-derived activity was mostly inhibited without any significant effect in peak I-derived activity, supporting APT1 as a major enzyme in peak II.

Immunohistochemical localization of ESD and APT1 in human pulmonary tissue. Fig. 6 shows representative immunohistochemical images of ESD and APT1 in human pulmonary tissue sections stained with anti-ESD antibody (A) and anti-APT1 antibody (B), respectively, using isotype antibody (C) as a negative control. As shown in Fig. 6A, ESD was highly expressed in the pulmonary epithelia with a strong dot-like or granular stain being localized in the cellular cytoplasm on the side of the luminal membrane. No obvious staining of ESD was observed in other tissue components. In Fig. 6B, APT1 was also

highly expressed in the pulmonary epithelia, with overall cellular staining including the cellular cytoplasm. Positive staining of APT1 was observed in the alveolar macrophages as well. In the case of the isotype antibody (Fig. 6C), there was little or no cross-reactivity with cell surface antigens on the tissue section.

DMD Fast Forward. Published on March 28, 2014 as DOI: 10.1124/dmd.114.057620
This article has not been copyedited and formatted. The final version may differ from this version.

Discussion

In this study, we have successfully identified two hydrolyzing enzymes, ESD and APT1, which would be primarily involved in the bioactivation of the anti-influenza prodrug LO in human pulmonary tissue, using a versatile methodology named proteomic correlation profiling (Kubota et al. 2009, McAllister and Gygi 2013, Sakurai et al. 2013). The proteomic correlation profiling has a feature to facilitate rapid identification of the responsible protein from crude complex lysate with fewer purification steps using a smaller starting material, as compared to the conventional methodology. Actually, in single-step gel filtration chromatography using only approximately 2.5 mg of the human pulmonary S9 fraction, we could identify two highly possible candidates of LO hydrolases, ESD for peak I and APT1 for peak II (Fig. 4).

ESD (EC 3.1.2.12), also known as S-formylglutathione hydrolase and methylumbelliferyl-acetate deacetylase, is a serine hydrolase that belongs to the esterase D family. This protein is expressed in the majority of normal tissues and is localized in the cytoplasm and cytoplasmic vesicles. ESD catalyzes the hydrolysis of S-formylglutathione, an intermediate of the glutathione-dependent pathway of formaldehyde detoxification, converting to the reduced forms of formic acid and glutathione (Eiberg et al. 1986, Harms et al. 1996). In addition, ESD can act as a carboxylesterase and hydrolyze a variety of ester substrates including O-acetylated sialic acids. For example, it has been reported that ESD can specifically cleave the O-acetyl ester linkage at the exocyclic C9 position of 9-O-acetyl-N-acetylneuraminic acid (Neu5, 9Ac2), suggesting that it is involved in the recycling of sialic acids (Varki et al. 1986). From a chemical structural point of view, LO

DMD Fast Forward. Published on March 28, 2014 as DOI: 10.1124/dmd.114.057620
This article has not been copyedited and formatted. The final version may differ from this version.

has an O-octanoyl ester linkage on its sialic acid-like structure which is very similar to that of Neu5, 9Ac2. This structural feature supports the reasonability of LO hydrolysis by ESD. In our experiment, recombinant ESD had distinct LO-hydrolyzing activity (Table 3), suggesting a responsible enzyme for LO hydrolysis. In addition, it was consistent with ESD as one of the LO hydrolases that the LO-hydrolyzing activity in pulmonary S9 was strongly inhibited by DFP, a serine hydrolase inhibitor (Fig. 2).

Similarly to ESD, sialate O-acetylesterase (SIAE) is known as an enzyme hydrolyzing O-acetyl ester linkage of Neu5, 9Ac2 (Schauer 2000, Angata et al. 2002). Moreover, ESD has been reported to show significant carboxylesterase activity against the following model substrates: α-naphthyl acetate and p-nitrophenyl acetate (Degrassi et al. 1999). A partial contribution of carboxylesterase on the LO hydrolysis was also supposed from the data that carboxylesterase inhibitor BNPP showed a weak inhibition against LO-hydrolyzing activity with 42.3% inhibition at the highest concentration (1 mM; Fig. 2). Considering these situations, we additionally investigated the potential of LO-hydrolyzing activities of SIAE and CES1, using their recombinant proteins. However, there was little or no LO-hydrolyzing activity in either protein (data not shown), indicating that these two enzymes were not responsible for the LO bioactivation although they were identified as candidate proteins for peak I and placed in a higher rank than ESD (Table 1). No LO-hydrolyzing activity was clearly observed in LTA4H as well, using its recombinant protein (data not shown). Nevertheless, the involvement of other enzyme(s) cannot be completely ruled out, since some proteins with hydrolase annotation still remain as candidate proteins for peak I, such as PGAM1, RCL, DDX39B, and IAH1. However, from enzyme activity using recombinant ESD (Table 3), it is highly plausible that ESD is at

DMD Fast Forward. Published on March 28, 2014 as DOI: 10.1124/dmd.114.057620
This article has not been copyedited and formatted. The final version may differ from this version.

least one of the component enzymes consisting of LO-hydrolyzing activity for peak I.

APT1 (EC 3.1.2.-), also known as lysophospholipase 1 (LYPLA1), is a serine hydrolase that belongs to the α/β hydrolase superfamily. This protein is expressed in various tissues including the gastrointestinal tract, respiratory epithelia, salivary gland, and liver, and is localized predominantly in the cytoplasm (Sugimoto et al. 1996, Wang et al. 1999, Hirano et al. 2009). APT1 works as a thioesterase that catalyzes depalmitoylation of H-Ras (Duncan et al. 1998), G protein α subunit (Duncan et al. 2002), and the endothelial isoform of nitric oxide synthase (Yeh et al. 1999). Furthermore, APT1 was also reported as an oxyesterase that cleaves the octanoyl group of ghrelin (Shanado et al. 2004, Satou et al. 2010). From the similarity of chemical structure with ghrelin, APT1 was hypothesized to be the most promising candidate for peak II, and this hypothesis was supported by LO-hydrolyzing activity of recombinant APT1 (Table 3). Moreover, as shown in Fig. 5, LO-hydrolyzing activity of peak II was almost inhibited by palmostatin B, a specific APT1 inhibitor (Dekker et al. 2010, Rusch et al. 2011). Also, in the same way as ESD, a strong enzyme inhibition by DFP (Fig. 2) was consistent with the fact that APT1 is categorized in the serine hydrolase class of enzymes. These results demonstrated that APT1 consisted mostly of active peak II.

Immunohistochemical analysis showed that ESD was highly localized in the cytoplasm and/or cytoplasmic vesicles of pulmonary epithelia (Fig. 6A), whereas APT1 was highly expressed in the overall pulmonary epithelia and alveolar macrophages (Fig. 6B). According to our previous reports, active metabolite laninamivir was highly maintained in the ELF and alveolar macrophages after inhaled administration of LO in healthy volunteers (Ishizuka et al. 2012). In addition, in mice intranasally administered LO,

DMD Fast Forward. Published on March 28, 2014 as DOI: 10.1124/dmd.114.057620
This article has not been copyedited and formatted. The final version may differ from this version.

the laninamivir was also deposited in the pulmonary tissue, especially in the epithelia. These results indicated that LO could be hydrolyzed into laninamivir in the pulmonary epithelia and/or alveolar macrophages, in which ESD and APT1 were mainly localized.

Prodrugs require bioactivation by the metabolizing enzymes in order to demonstrate its therapeutic effect. Genetic polymorphism in the prodrug-activating enzymes can cause a crucial impact on the interindividual variability in the drug exposure and response, as reported in some drugs, such as clopidogrel (Shuldiner et al. 2009), codeine (VanderVaart et al. 2011), and tramadol (Gan et al. 2007). Regarding the LO-hydrolyzing enzymes, the genetic polymorphism has been identified for ESD in a previous report (Ebeli-Struijk et al. 1976), in which the ESD*2 allele was commonly observed with a different gene frequency depending on ethnic groups. Additionally, it has been reported that the enzyme activity associated with ESD*2 was estimated to be 40% lower than that associated with ESD*1, using a typical substrate 4-methylumbelliferyl acetate (Horai and Matsunaga 1984). However, in the case of LO, this genetic factor would be unlikely to make a huge influence on the interindividual variability, since at least the two enzymes (ESD and APT1) were involved in the LO bioactivation and the contribution of multiple enzymes in the same reaction is considered to dilute the potential impact on the interindividual variability. Further assessment on this issue should be performed more precisely in the future.

In conclusion, this study demonstrated that both ESD and APT1 would be key enzymes responsible for the bioactivation of LO in the human pulmonary tissue. These enzymes could play an important role for exhibiting anti-influenza virus activity when LO reached the respiratory tract after inhaled administration in humans.

Acknowledgements

We gratefully acknowledge Hidetaka Sakurai and Hiroshi Katsuno for experimental suggestions and contributions to this work. We also appreciate Dr. Makoto Yamashita for many helpful discussions.

Authorship Contributions

Participated in research design: Koyama, Ogura, Nakai, and Kubota

Conducted experiments: Koyama, Ogura, Watanabe, and Oofune

Contributed new reagents or analytical tools: Koyama and Ogura

Performed data analysis: Koyama, Ogura, and Munemasa

Wrote or contributed to the writing of manuscript: Koyama, Ogura, Nakai, Kubota, Shinagawa, and Izumi

References

Angata T, Varki A (2002) Chemical diversity in the sialic acids and related alpha-keto acids: an evolutionary perspective. *Chem Rev* **102**: 439–469.

Cox J, Matic I, Hilger M, Nagaraj N, Selbach M, Olsen JV, Mann M (2009) A practical guide to the MaxQuant computational platform for SILAC-based quantitative proteomics. *Nat Protoc* **4**: 698–705.

Cox J, Neuhauser N, Michalski A, Scheltema RA, Olsen JV, Mann M (2011) Andromeda: a peptide search engine integrated into the MaxQuant environment. *J Proteome Res* **10**: 1794–1805.

Degrassi G, Uotila L, Klima R, Venturi V (1999) Purification and properties of an esterase from the yeast Saccharomyces cerevisiae and identification of the encoding gene. *Appl Environ Microbiol* **65**: 3470–3472.

Dekker FJ, Rocks O, Vartak N, Menninger S, Hedberg C, Balamurugan R, Wetzel S, Renner S, Gerauer M, Schölermann B, Rusch M, Kramer JW, Rauh D, Coates GW, Brunsveld L, Bastiaens PI, Waldmann H (2010) Small-molecule inhibition of APT1 affects Ras localization and signaling. *Nat Chem Biol* **6**: 449–456.

Duncan JA, Gilman AG (1998) A cytoplasmic acyl-protein thioesterase that removes palmitate from G protein alpha subunits and p21(RAS). *J Biol Chem* **273**: 15830–15837.

Duncan JA, Gilman AG (2002) Characterization of Saccharomyces cerevisiae acyl-protein thioesterase 1, the enzyme responsible for G protein alpha subunit deacylation in vivo. *J Biol Chem* **277**: 31740–31752.

Ebeli-Struijk AC, Wurzer-Figurelli EM, Ajmar F, Meera Khan P (1976) The distribution of esterase D variants in different ethnic groups. *Hum Genet* **34**: 299–306.

Eiberg H, Mohr J (1986) Identity of the polymorphisms for esterase D and S-formylglutathione hydrolase in red blood cells. *Hum Genet* **74**: 174–175.

Gan SH, Ismail R, Wan Adnan WA, Zulmi W (2007) Impact of CYP2D6 genetic polymorphism on tramadol pharmacokinetics and pharmacodynamics. *Mol Diagn Ther* **11**: 171–181.

Gerber SA, Rush J, Stemman O, Kirschner MW, Gygi SP (2003) Absolute quantification of proteins and phosphoproteins from cell lysates by tandem MS. *Proc Natl Acad Sci U S A* **100**: 6940–6945.

Harms N, Ras J, Reijnders WN, van Spanning RJ, Stouthamer AH (1996) S-formylglutathione hydrolase of Paracoccus denitrificans is homologous to human esterase D: a universal pathway for formaldehyde detoxification? *J Bacteriol* **178**: 6296–6299.

Hirano T, Kishi M, Sugimoto H, Taguchi R, Obinata H, Ohshima N, Tatei K, Izumi T (2009) Thioesterase activity and subcellular localization of acylprotein thioesterase 1/lysophospholipase 1. *Biochim Biophys Acta* **1791**: 797–805.

Horai S, Matsunaga E (1984) Differential enzyme activities in human esterase D phenotypes. *Hum Genet* **66**: 168–170.

Ishizuka H, Yoshiba S, Okabe H, Yoshihara K (2009) Clinical pharmacokinetics of R-125489, a novel long-acting neuraminidase inhibitor, after single and multiple inhaled doses of its prodrug, CS-8958, in healthy male volunteers. *J Clin Pharmacol* **50**: 1319–1329.

Ishizuka H, Toyama K, Yoshiba S, Okabe H, Furuie H (2012) Intrapulmonary distribution and pharmacokinetics of laninamivir, a neuraminidase inhibitor, after a single inhaled administration of its prodrug, laninamivir octanoate, in healthy volunteers. *Antimicrob Agents Chemother* **56**: 3873–3878.

Kashiwagi S, Watanabe A, Ikematsu H, Awamura S, Okamoto T, Uemori M, Ishida K (2013) Laninamivir octanoate for post-exposure prophylaxis of influenza in household contacts: a randomized double blind placebo controlled trial. *J Infect Chemother* **19**: 740–749.

Koyama K, Takahashi M, Oitate M, Nakai N, Takakusa H, Miura SI, Okazaki O (2009) CS-8958, a prodrug of the novel neuraminidase inhibitor R-125489, demonstrates a favorable long retention profile in the mouse respiratory tract. *Antimicrob Agents Chemother* **53**: 4845–4851.

Koyama K, Takahashi M, Nakai N, Takakusa H, Murai T, Hoshi M, Yamamura N, Kobayashi N, Okazaki O (2010) Pharmacokinetics and disposition of CS-8958, a long-acting prodrug of the novel neuraminidase inhibitor laninamivir in rats. *Xenobiotica* **40**: 207–216.

Koyama K, Nakai D, Takahashi M, Nakai N, Kobayashi N, Imai T, Izumi T (2013) Pharmacokinetic mechanism involved in the prolonged high retention of laninamivir in mouse respiratory tissues after intranasal administration of its prodrug laninamivir octanoate. *Drug Metab Dispos* **41**: 180–187.

Kubota K, Anjum R, Yu Y, Kunz RC, Andersen JN, Kraus M, Keilhack H, Nagashima K, Krauss S, Paweletz C, Hendrickson RC, Feldman AS, Wu CL, Rush J, Villén J, Gygi SP (2009) Sensitive multiplexed analysis of kinase activities and activity-based

kinase identification. *Nat Biotechnol* **27**: 933–940.

McAllister FE, Gygi SP (2013) Correlation profiling for determining kinase-substrate relationships. *Methods* **61**: 227–235.

Ong SE, Blagoev B, Kratchmarova I, Kristensen DB, Steen H, Pandey A, Mann M (2002) Stable isotope labeling by amino acids in cell culture, SILAC, as a simple and accurate approach to expression proteomics. *Mol Cell Proteomics* **1**: 376–386.

Rappsilber J, Mann M, Ishihama Y (2007) Protocol for micro-purification, enrichment, pre-fractionation and storage of peptides for proteomics using StageTips. *Nat Protoc* **2**: 1896–1906.

Rautio J, Kumpulainen H, Heimbach T, Oliyai R, Oh D, Järvinen T, Savolainen J (2008) Prodrugs: design and clinical applications. *Nat Rev Drug Discov* **7**: 255–270.

Ross PL, Huang YN, Marchese JN, Williamson B, Parker K, Hattan S, Khainovski N, Pillai S, Dey S, Daniels S, Purkayastha S, Juhasz P, Martin S, Bartlet-Jones M, He F, Jacobson A, Pappin DJ (2004) Multiplexed protein quantitation in Saccharomyces cerevisiae using amine-reactive isobaric tagging reagents. *Mol Cell Proteomics* **3**: 1154–1169.

Rusch M, Zimmermann TJ, Bürger M, Dekker FJ, Görmer K, Triola G, Brockmeyer A, Janning P, Böttcher T, Sieber SA, Vetter IR, Hedberg C, Waldmann H (2011) Identification of acyl protein thioesterases 1 and 2 as the cellular targets of the Ras-signaling modulators palmostatin B and M. *Angew Chem Int Ed Engl* **50**: 9838–9842.

Sakurai H, Kubota K, Inaba S, Takanaka K, Shinagawa A (2013) Identification of a metabolizing enzyme in human kidney by proteomic correlation profiling. *Mol Cell*

Proteomics **12**: 2313–2323.

Satou M, Nishi Y, Yoh J, Hattori Y, Sugimoto H (2010) Identification and characterization of acyl-protein thioesterase 1/lysophospholipase I as a ghrelin deacylation/lysophospholipid hydrolyzing enzyme in fetal bovine serum and conditioned medium. *Endocrinology* **151**: 4765–4775.

Schauer R (2000) Achievements and challenges of sialic acid research. *Glycoconj J* **17**: 485–499.

Shanado Y, Kometani M, Uchiyama H, Koizumi S, Teno N (2004) Lysophospholipase I identified as a ghrelin deacylation enzyme in rat stomach. *Biochem Biophys Res Commun* **325**: 1487–1494.

Shuldiner AR, O'Connell JR, Bliden KP, Gandhi A, Ryan K, Horenstein RB, Damcott CM, Pakyz R, Tantry US, Gibson Q, Pollin TI, Post W, Parsa A, Mitchell BD, Faraday N, Herzog W, Gurbel PA (2009) Association of cytochrome P450 2C19 genotype with the antiplatelet effect and clinical efficacy of clopidogrel therapy. *JAMA* **302**: 849–857.

Sugaya N, Ohashi Y (2010) Long-acting neuraminidase inhibitor laninamivir octanoate (CS-8958) versus oseltamivir as treatment for children with influenza virus infection. *Antimicrob Agents Chemother* **54**: 2575–2582.

Sugimoto H, Hayashi H, Yamashita S (1996) Purification, cDNA cloning, and regulation of lysophospholipase from rat liver. *J Biol Chem* **271**: 7705–7711.

VanderVaart S, Berger H, Sistonen J, Madadi P, Matok I, Gijsen VM, de Wildt SN, Taddio A, Ross CJ, Carleton BC, Hayden MR, Koren G (2011) CYP2D6 polymorphisms and codeine analgesia in postpartum pain management: a pilot study.

Ther Drug Monit **33**: 425–432.

Varki A, Muchmore E, Diaz S (1986) A sialic acid-specific O-acetylesterase in human erythrocytes: possible identity with esterase D, the genetic marker of retinoblastomas and Wilson disease. *Proc Natl Acad Sci U S A* **83**: 882–886.

Wang A, Yang HC, Friedman P, Johnson CA, Dennis EA (1999) A specific human lysophospholipase: cDNA cloning, tissue distribution and kinetic characterization. *Biochim Biophys Acta* **1437**: 157–169.

Watanabe A, Chang SC, Kim MJ, Chi DW, Ohashi Y (2010) Long-acting neuraminidase inhibitor laninamivir octanoate versus oseltamivir for treatment of influenza: a double-blind, randomized, noninferiority clinical trial. *Clin Infect Dis* **51**: 1167–1175.

Watanabe A (2013) A randomized double-blind controlled trial of laninamivir compared with oseltamivir for the treatment of influenza in patients with chronic respiratory diseases. *J Infect Chemother* **19**: 98–102.

Wessel D, Flügge UI (1984) A method for the quantitative recovery of protein in dilute solution in the presence of detergents and lipids. *Anal Biochem* **138**: 141–143.

Yamashita M, Tomozawa T, Kakuta M, Tokumitsu A, Nasu H, Kubo S (2009) CS-8958, a prodrug of the new neuraminidase inhibitor R-125489, shows long-acting anti-influenza virus activity. *Antimicrob Agents Chemother* **53**: 186–192.

Yeh DC, Duncan JA, Yamashita S, Michel T (1999) Depalmitoylation of endothelial nitric-oxide synthase by acyl-protein thioesterase 1 is potentiated by Ca(2+)-calmodulin. *J Biol Chem* **274**: 33148–33154.

Yoshiba S, Okabe H, Ishizuka H (2011) Pharmacokinetics of laninamivir after a single administration of its prodrug, laninamivir octanoate, a long-acting neuraminidase

inhibitor, using an easy-to-use inhaler in healthy volunteers. *J Bioequiv Availab* **3**: 1–4.

Zawilska JB, Wojcieszak J, Olejniczak AB (2013) Prodrugs: a challenge for the drug development. *Pharmacol Rep* **65**: 1–14.

Footnotes

Kumiko Koyama and Yuji Ogura contributed equally to this work and should be considered as joint first authors.

Figure legends

Figure 1. Chemical structures of laninamivir octanoate (LO) and its active metabolite laninamivir.

After inhaled administration of LO in humans, the active metabolite laninamivir is generated by an enzymatic hydrolysis of the octanoyl ester moiety. When dissolved in water, LO is equilibrated at 9:1 (3-acyl form:2-acyl form) and therefore defined as a mixture of the 3-acyl form (major) and the 2-acyl form (minor).

Figure 2. Enzymatic LO hydrolysis in human pulmonary subcellular fractions.

A, shows LO-hydrolyzing activity in human pulmonary subcellular fractions (S9, cytosol, and microsomes). Each data represents the mean±S.E. in triplicate determinations. B, shows the inhibitory effect of typical esterase inhibitors on LO-hydrolyzing activity in human pulmonary S9. Each data represents the mean of triplicate determinations.

Figure 3. A schematic diagram of proteomic correlation profiling to identify the candidates for LO-hydrolyzing enzymes.

Figure 4. Selection of possible candidate proteins demonstrating LO-hydrolyzing activity in human pulmonary tissue.

After fractionation of 105,000 *g* supernatant of NP-40 treated human pulmonary S9 by gel filtration chromatography, an aliquot of each fraction was assayed for the LO-hydrolyzing activity (solid line, left y-axis) and protein concentration (open bar, right y-axis). The

positions of the native molecular weight markers are indicated at the bottom.

Figure 5. Inhibitory effect of palmostatin B on LO-hydrolyzing activity in the fractions eluted from gel filtration chromatography.

An aliquot of each fraction was assayed for LO-hydrolyzing activity in the absence and presence of a specific APT1 inhibitor, palmostatin B (0.1 μM). The positions of the native molecular weight markers are indicated at the bottom.

Figure 6. Representative immunohistochemical images of ESD and APT1 in human pulmonary tissue.

Human pulmonary tissue sections were stained with anti-ESD antibody (A), anti-APT1 antibody (B), and isotype control (C). After treatment with HPR-labeled anti-rabbit IgG, the antibody complex was visualized as a dark brown precipitate by using DAB as a substrate.

DMD Fast Forward. Published on March 28, 2014 as DOI: 10.1124/dmd.114.057620
This article has not been copyedited and formatted. The final version may differ from this version.

Table 1. Correlation between relative intensity of identified proteins and LO-hydrolyzing active peak I (fraction No. 26-32) on gel filtration chromatogram.

Rank	Uniprot ID	Protein description	Gene name	Correlation coefficient	
1	Q96G03	Phosphoglucomutase-2	PGM2	0.9966	
2	Q9UBQ7	Glyoxylate reductase/hydroxypyruvate reductase	GRHPR	0.9963	
3	P18669	Phosphoglycerate mutase 1	PGAM1	0.9953	*
4	P62495	Eukaryotic peptide chain release factor subunit 1	ETF1	0.9930	
5	P36955	Pigment epithelium-derived factor	SERPINF1	0.9824	
6	Q9HAT2	Sialate O-acetylesterase	SIAE	0.9815	*
7	P35270	Sepiapterin reductase	SPR	0.9758	
8	O75131	Copine-3	CPNE3	0.9741	
9	Q99798	Aconitate hydratase, mitochondrial	ACO2	0.9736	
10	O60888	Protein CutA	CUTA	0.9728	
11	Q99729	Heterogeneous nuclear ribonucleoprotein A/B	HNRNPAB	0.9714	
12	P09960	Leukotriene A-4 hydrolase	LTA4H	0.9703	*
13	O76003	Glutaredoxin-3	GLRX3	0.9693	
14	P23141	Liver carboxylesterase 1	CES1	0.9653	*
15	O43598	Deoxyribonucleoside 5-monophosphate N-glycosidase	RCL	0.9632	*
16	Q13838	Spliceosome RNA helicase DDX39B	DDX39B	0.9602	*
17	P40926	Malate dehydrogenase, mitochondrial	MDH2	0.9599	
18	Q9H0R4	Haloacid dehalogenase-like hydrolase domain-containing protein 2	HDHD2	0.9578	
19	O15305	Phosphomannomutase 2	PMM2	0.9575	
20	P21695	Glycerol-3-phosphate dehydrogenase [NAD(+)], cytoplasmic	GPD1	0.9519	
21	Q9Y3F4	Serine-threonine kinase receptor-associated protein	STRAP	0.9478	
22	P13284	Gamma-interferon-inducible lysosomal thiol reductase	IFI30	0.9458	
23	P10768	S-formylglutathione hydrolase	ESD	0.9432	*
24	P49407	Beta-arrestin-1	ARRB1	0.9432	
25	Q2TAA2	Isoamyl acetate-hydrolyzing esterase 1 homolog	IAH1	0.9430	*
26	P14866	Heterogeneous nuclear ribonucleoprotein L	HNRNPL	0.9427	
27	Q0VGL1	UPF0539 protein C7orf59	C7orf59	0.9427	
28	Q9BUJ2	Heterogeneous nuclear ribonucleoprotein U-like protein 1	HNRNPUL 1	0.9389	
29	Q9UHA4	Ragulator complex protein LAMTOR3	LAMTOR3	0.9340	
30	Q13813	Spectrin alpha chain, brain	SPTAN1	0.9333	

Among the 1160 proteins identified, the top 30 candidates with high correlation coefficient between relative intensity of the identified proteins and LO-hydrolyzing active peak I (fraction No. 26-32) on gel filtration chromatogram are listed above. The asterisk represents hydrolase domain which was annotated by Uniprot. Identified peptides for each protein are listed in Supplemental Table 1.

DMD Fast Forward. Published on March 28, 2014 as DOI: 10.1124/dmd.114.057620
This article has not been copyedited and formatted. The final version may differ from this version.

Table 2. Correlation between relative intensity of identified proteins and LO-hydrolyzing active peak II (fraction No. 33-39) on gel filtration chromatogram.

Rank	Uniprot ID	Protein description	Gene name	Correlation coefficient	
1	Q01995	Transgelin	TAGLN	0.9982	
2	Q8WWI1	LIM domain only protein 7	LMO7	0.9978	
3	Q9UIJ7	GTP:AMP phosphotransferase, mitochondrial	AK3	0.9974	
4	P80188	Neutrophil gelatinase-associated lipocalin	LCN2	0.9971	
5	Q9UL25	Ras-related protein Rab-21	RAB21	0.9960	
6	Q9Y281	Cofilin-2	CFL2	0.9955	
7	P43034	Platelet-activating factor acetylhydrolase IB subunit alpha	PAFAH1B1	0.9953	
8	P22061	Protein-L-isoaspartate(D-aspartate) O-methyltransferase	PCMT1	0.9953	
9	Q15907	Ras-related protein Rab-11B;Ras-related protein Rab-11A	RAB11B	0.9943	
10	P00568	Adenylate kinase isoenzyme 1	AK1	0.9935	
11	Q9Y2Q3	Glutathione S-transferase kappa 1	GSTK1	0.9896	
12	P11234	Ras-related protein Ral-B	RALB	0.9879	
13	P61106	Ras-related protein Rab-14	RAB14	0.9873	
14	Q15493	Regucalcin	RGN	0.9871	
15	Q9NRV9	Heme-binding protein 1	HEBP1	0.9867	
16	P07996	Thrombospondin-1	THBS1	0.9867	
17	P00915	Carbonic anhydrase 1	CA1	0.9867	
18	Q6IBS0	Twinfilin-2	TWF2	0.9860	
19	P52566	Rho GDP-dissociation inhibitor 2	ARHGDIB	0.9844	
20	O75367	Core histone macro-H2A.1	H2AFY	0.9841	
21	P46777	60S ribosomal protein L5	RPL5	0.9839	
22	P12814	Alpha-actinin-1	ACTN1	0.9838	
23	P25774	Cathepsin S	CTSS	0.9823	*
24	P00918	Carbonic anhydrase 2	CA2	0.9819	
25	P09382	Galectin-1	LGALS1	0.9813	
26	O75608	Acyl-protein thioesterase 1	APT1	0.9765	*
27	Q6FI81	Anamorsin	CIAPIN1	0.9753	
28	Q13938	Calcyphosin	CAPS	0.9744	
29	Q05315	Eosinophil lysophospholipase	CLC	0.9743	*
30	Q15717	ELAV-like protein 1	ELAVL1	0.9736	

Among the 1003 proteins identified, the top 30 candidates with high correlation coefficient between relative intensity of the identified proteins and LO-hydrolyzing active peak II (fraction No. 33-39) on gel filtration chromatogram are listed above. The asterisk represents hydrolase domain which was annotated by Uniprot. Identified peptides for each protein are listed in Supplemental Table 2.

Table 3. LO-hydrolyzing activity of recombinant ESD and APT1.

Enzyme source	LO-hydrolyzing activity
	pmol/min/mg
Pulmonary S9	1.56±0.05
rESD	232±16
rAPT1	377±36
BSA	0.105±0.022

Candidate protein recombinants (rESD and rAPT1), pulmonary S9, and BSA (negative control) were incubated with 10 μM LO, and the enzyme activity was tested. Each value represents the mean±S.E. in triplicate determinations.

Fig. 1

Laninamivir octanoate (LO)

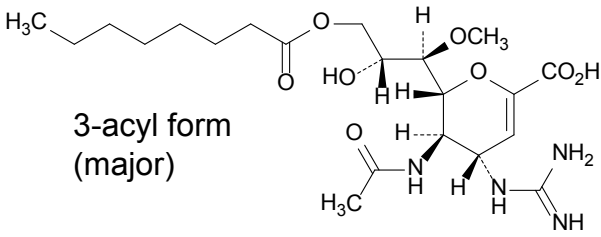

3-acyl form
(major)

and

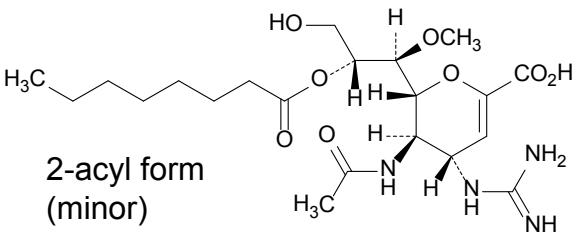

2-acyl form
(minor)

Laninamivir

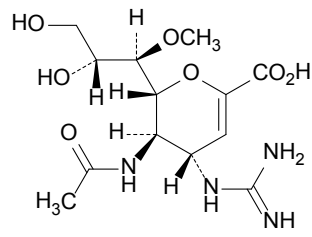

Fig. 2

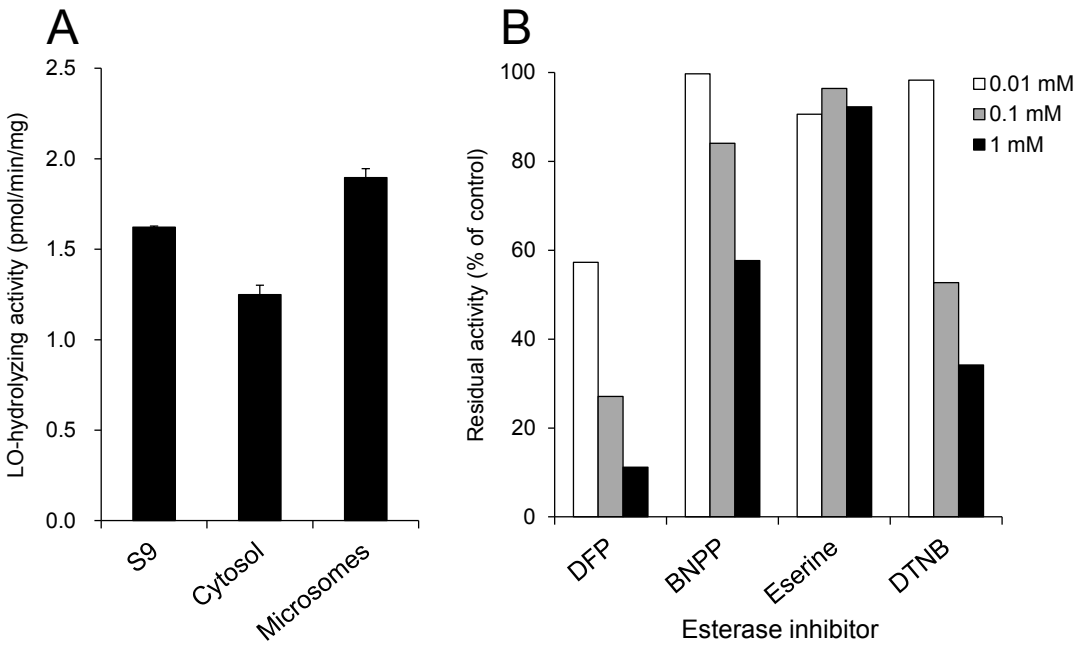
A
LO-hydrolyzing activity (pmol/min/mg)
2.5
2.0
1.5
1.0
0.5
0.0
S9
Cytosol
Microsomes
B
Residual activity (% of control)
100
80
60
40
20
0
0.01 mM
0.1 mM
1 mM
DFP
BNPP
Eserine
DTNB
Esterase inhibitor

Fig. 3

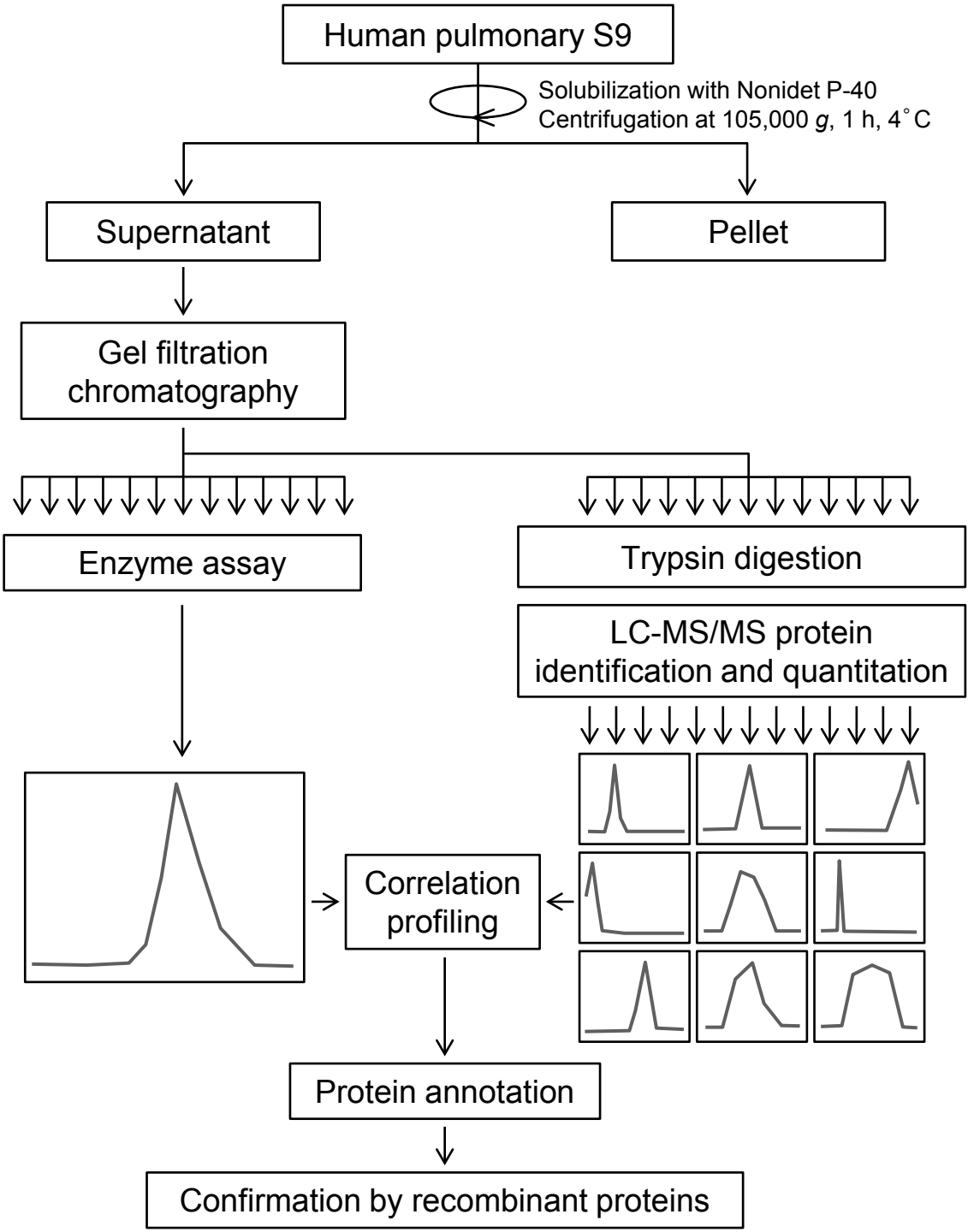
Human pulmonary S9
Solubilization with Nonidet P-40
Centrifugation at 105,000 g, 1 h, 4˚C
Supernatant
Pellet
Gel filtration chromatography
Enzyme assay
Trypsin digestion
LC-MS/MS protein identification and quantitation
Correlation profiling
Protein annotation
Confirmation by recombinant proteins

Fig. 4

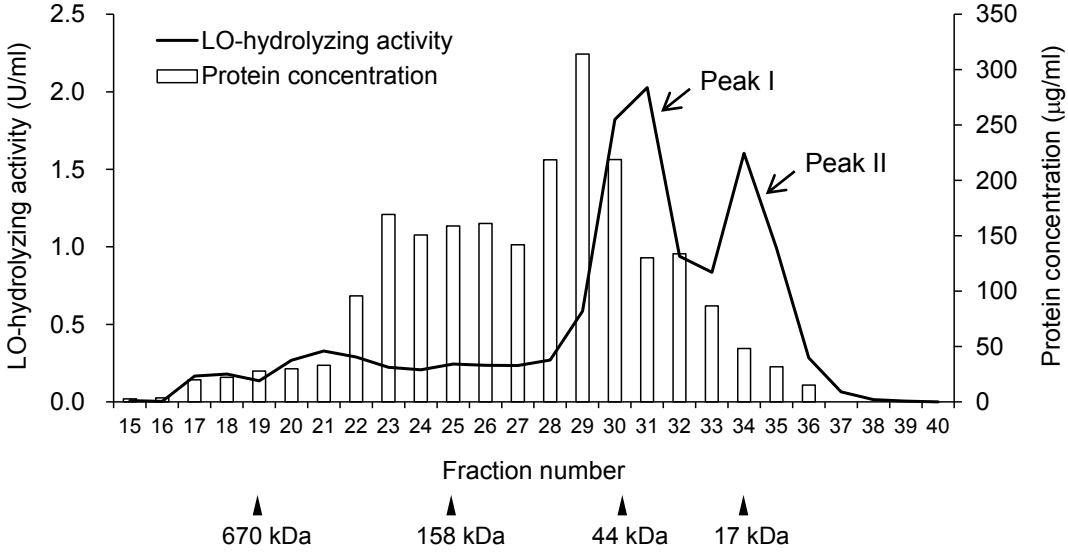
LO-hydrolyzing activity
Protein concentration
Peak I
Peak II
LO-hydrolyzing activity (U/ml)
Protein concentration (μg/ml)
Fraction number
670 kDa
158 kDa
44 kDa
17 kDa

Fig. 5

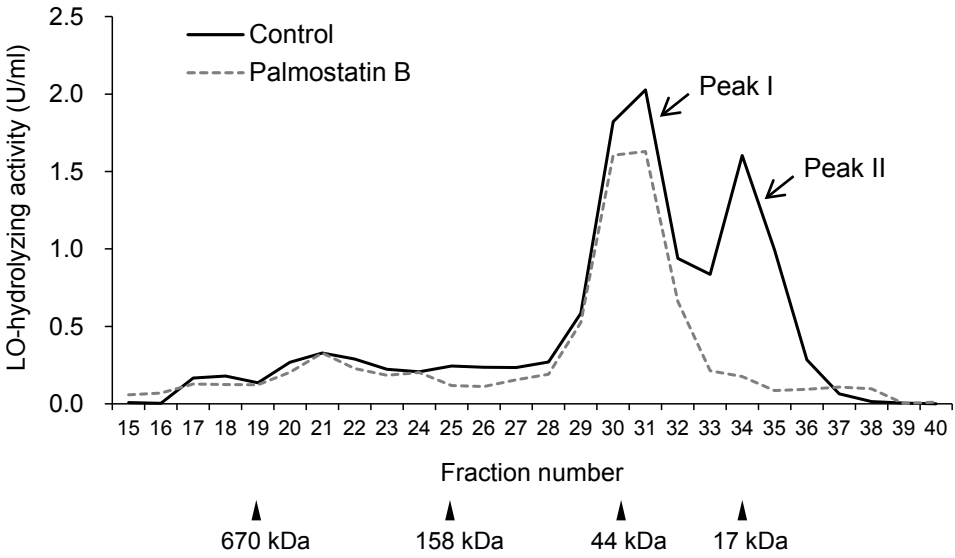
Control
Palmostatin B
Peak I
Peak II
LO-hydrolyzing activity (U/ml)
2.5
2.0
1.5
1.0
0.5
0.0
15 16 17 18 19 20 21 22 23 24 25 26 27 28 29 30 31 32 33 34 35 36 37 38 39 40
Fraction number
670 kDa
158 kDa
44 kDa
17 kDa

Fig. 6